J Radioanal Nucl Chem (2011) 287:847–852
DOI 10.1007/s10967-010-0889-6

Synthesis and biodistribution of a novel ^{99m}Tc complex of HYNIC-conjugated metronidazole as a potential tumor hypoxia imaging agent

Liqin Liu · Min Zhang · Guangrong Zhong · Xuebin Wang

Received: 30 August 2010 / Published online: 2 November 2010

Abstract A conjugate of 6-hydrazinopyridine-3-carboxylic acid (HYNIC) with the amino analogue of metronidazole (MN) was synthesized through a multiple-step reaction. HYNIC-MN could be labeled easily and efficiently with ^{99m}Tc using *N*-(2-hydroxy-1,1-bis(hydroxymethyl)ethyl)glycine (tricine) and ethylenediamine -*N*,*N*′-diacetic acid (EDDA) as coligands to form the ^{99m}Tc–HYNIC–MN complex in high yield (>95%). Its partition coefficient indicated that it was a good hydrophilic complex. The tumor cell experiment showed that the ^{99m}Tc–HYNIC–MN complex had a certain hypoxic selectivity. The biodistribution studies of ^{99m}Tc–HYNIC–MN in Kunming mice bearing S180 tumor showed a favorable tissue distribution profile with high tumor uptake, and low or negligible accumulation in non-target organs, suggesting ^{99m}Tc–HYNIC–MN would be a novel potential tumor hypoxia imaging agent.

Keywords ^{99m}Tc · HYNIC · Bifunctional chelator · Hypoxia imaging agent · Metronidazole

L. Liu (✉) · M. Zhang · G. Zhong
Department of Biological Science and Engineering, School of Chemical and Biological Engineering, University of Science and Technology Beijing, 30th Xueyuan Road, Haidian District, Beijing 100083, People's Republic of China
e-mail: liuliqin@ustb.edu.cn

X. Wang
Key Laboratory of Radiopharmaceuticals (Beijing Normal University), Ministry of Education, College of Chemistry, Beijing Normal University, Beijing 100875, People's Republic of China

Introduction

The existence of hypoxic cells in tumors [1] has long been recognized as a major problem in radiotherapy [2] and is also a potential problem in the chemotherapy [3] of cancer. The identification and quantitative estimation of tumor hypoxia becomes an important factor in planning the therapeutic strategy for a better clinical outcome. So it is important to detect hypoxia within tumors. Many invasive methods have been developed for the measurement of hypoxia, but none of these is in conventional clinical use owing to their invasive nature, incommodiousness, and incapability to acquire repeated measures. Nuclear medicine offers a non-invasive method for detecting tumor hypoxia [4]. Compounds that are selectively accumulated in hypoxic tissue may be labeled with radionuclides either positron-emitting or single photon gamma. Up to now, almost all of the radiolabeled probes for hypoxic cells have been based on nitroimidazoles derivatives [5] which are enzymatically reduced and accumulated in hypoxic regions. Because of the advantageous characteristics of ^{99m}Tc (ideal half-life, optimal γ-energy, low cost and good availability), research has mainly focused on ^{99m}Tc labeled hypoxia imaging agents. Recently, several ^{99m}Tc labeled nitroimidazole analogues have been reported [6–12]. However, these hypoxia imaging agents have the common defects of the relative lower tumor uptakes and slow clearance from blood. So it is very interesting and necessary to search for an ideal hypoxia imaging agent. In this study, 6-hydrazinopyridine-3-carboxylic acid (HYNIC) were chosen as chelating sites because they have been widely used for ^{99m}Tc labeling of proteins and peptides on the basis of different coligands [13–16] and conjugated to 2-methyl-5-nitro-1-[2-aminoethyl]imidazole (MN-NH_2). ^{99m}Tc–HYNIC–MN was prepared by coordination with

^{99m}Tc, and their properties in vitro and in vivo were studied and evaluated as a potential tumor hypoxic imaging agent. To the best of our knowledge, this is the first report using the HYNIC-MN in the preparation of ^{99m}TcO complex as tumor hypoxia imaging agent.

Experimental

Materials

1,3-Dicyclohexylcarbodiimide (DCC), sulfo-*N*-hydroxy succinimide (NHS) and metronidazole (MN) were purchased from Aldrich Chemical Co. Other chemicals were purchased from Acros Chemical Co. ^{1}H NMR spectra were collected on a Bruker 500 MHz FT-NMR spectrometer. ESI–MS were performed on API-3000 LC/MS. $Na^{99m}TcO_4$ was obtained from a commercial ^{99}Mo/^{99m}Tc generator, Beijing Atomic High-tech Co. Kunming mice (weighing 20–25 g) was obtained from the Animal Center of Peking University.

Preparation and structure confirmation of unlabeled HYNIC–MN

6-(*Tert*-butoxycarbonyl)-hydrazinopyridine-3-carboxylic acid (Boc-HYNIC) and 2-methyl-5-nitro-1-[2-aminoethyl]imidazole (MN-NH_2) were synthesized according to procedures described elsewhere [17, 3].

2-Methyl-5-nitro-1-imidazole ethylamine (MN-NH_2) (0.41 g, 2.6 mmol) was dissolved in 10 mL dry DMF, then 6-Boc-hydrazinopyridine-3-carboxylic acid (Boc-HYNIC) (0.72 g, 2.7 mmol) and NHS (0.30 g, 2.6 mmol) were added. The solution was cooled to 0 °C and DCC (0.54 g, 2.6 mmol) was added. The reaction mixture was stirred for 30 min at 0 °C and then over night at room temperature. White precipitate was removed by filtration. Next, the solvent was evaporated under reduced pressure giving the crude product. After purification by column chromatography using a dichloromethane:methanol (30:1, v/v) solvent system, the solvent was removed under reduced pressure to provide 2-methyl-5-nitro-1-[2-(6-Boc-hydrazinopyridine-3-carbonyl)amino] ethyl imidazole (Boc–HYNIC–MN, 0.59 g, 56.2%) as white crystals. ^{1}H NMR ($CDCl_3$) δ: 8.45 (s, 1H), 7.93 (s, 1H), 7.88 (d, 1H), 7.28 (s, 1H), 7.07 (s, 1H), 6.66 (d, 1H), 4.57 (t, 1H), 3.77 (t, 8H), 2.48 (s, 3H), 2.18 (d, 3H),1.47 (m, 9H); MS (ESI): $[M + H]^+$ 406.6.

Boc–HYNIC–MN (0.20 g, 0.5 mmol) was stirred in 100% TFA (7.0 mL) for 10 min at room temperature. After removal of the solvent under reduced pressure, the reside was washed with dry ether to produce 2-methyl-5-nitro-1-[2-(6-hydrazinopyridine-3-carbonyl)amino]ethyl imidazole (HYNIC–MN) quantitatively as white crystals. ^{1}H NMR (D_2O) δ: 8.30 (s, 1H), 8.11 (s, 1H), 7.87 (m, 1H), 6.86 (d, 1H), 4.63 (t, 2H), 3.75 (t, 2H), 2.60 (s, 3H); MS (ESI): $[M + H]^+$ 306.5.

Labeling of HYNIC–MN

Labeling of HYNIC–MN with ^{99m}Tc was performed by addition of 1 mL of sodium pertechnetate solution (1.85–185 MBq) to a vial containing HYNIC-MN (10 μg), tricine (60 mg) and EDDA (5 mg) and 0.2 mL saline, then sodium hydroxide was added to adjust the pH value to 7. $SnCl_2$ solution (25 μg) was added and the vial was kept at 100 °C for 15 min.

Radiochemical purity analysis

The final complexes were analyzed by TLC and HPLC for the radiochemical purity (RCP). The TLC was performed on a polyamide strip and eluted with saline. The reaction mixture was spotted on the start line, then the strip was developed using saline as a developing system. The strips were removed, dried, cut to 1 cm segments, and assayed for the radioactivity using a well-type γ-scintillation counter.

HPLC analysis was carried out with a reversed-phase column (Kromasil 100-5C, 250 × 4.6 mm^2), Shimadzu SCL-10AVP series. The flow rate was 1 mL/min. The mobile phase was isocratic with 80% solvent A (25 mM NH_4OAc buffer, pH 5.0) and 20% solvent B (acetonitrile) at 0–2 min, followed by a gradient mobile phase going from 20% solvent B at 2 min to 25% solvent B at 5 min and to 30% solvent B at 20 min.

Stability test

The stability of ^{99m}Tc–HYNIC–MN was studied by measuring RCP of the final complexes by HPLC at different times after preparation.

Determination of the partition coefficient (log *P*) for the complex

The partition coefficient was determined by mixing the complex with an equal volume of 1-octanol and phosphate buffer (0.025 mol/L, pH 7.4) in a centrifuge tube. The mixture was vortexed at room temperature for 1 min and then centrifuged at 5,000 rpm for 5 min. From the 1-octanol phase and the water phase, 0.1 mL of aliquot was removed and counted in a well γ-counter respectively. Each measurement was repeated three times. Care was taken to avoid cross contamination between the phases. The partition coefficient *P* was calculated using the following equation:

$$P = (\text{cpm in octanol} - \text{cpm in background})/(\text{cpm in buffer} - \text{cpm in background})$$

Usually the final partition coefficient value was expressed as log P.

Paper electrophoresis

1 μL sample was spotted on a piece of Whatman 1 chromatography paper, saturated with 0.05 M pH 7.4 phosphate buffer, in an electrophoresis bath. Across 12 cm of the strip, 150 V was applied for 1.5 h. The strips were dried, and the distribution of radioactivity on the strip was determined.

Cellular accumulation

The complex was in vitro evaluated according to the previous method [11, 12]. S180 cells were suspended in fresh DMEM growth medium at a cell concentration of 2×10^6 cells/mL. Aliquots of 20 mL were placed in glass vials and incubated at 37 °C with gentle stirring under an atmosphere of 95% air plus 5% carbon dioxide (aerobic exposure) or 95% nitrogen plus 5% carbon dioxide (hypoxic exposure, oxygen concentration <10 ppm). After a 30–45 min equilibration period, 0.3 mL of ^{99m}Tc–HYNIC–MN was added to each vial at a final activity of approximately 0.25 MBq/mL and a drug concentration of approximately 0.7 μg/mL. The 0.9 mL samples were removed at various time intervals. From each sample, the 0.2 mL sample was centrifuged at 1,500 rpm for 5 min. A 90 μL aliquot of the supernatant was removed for counting, and the left sample containing cells and 110 μL medium was also counted. The ratio of the radioactivity in the cell pellet to that in the supernatant medium (C_{in}/C_{out}) was calculated as (residue counts − supernatant counts)/supernatant counts. At each time point, five samples were determined. During the whole procedure, the cells' viability was more than 90%.

Biodistribution studies in mice

Biodistribution studies were performed in healthy Kunming mice and Kunming mice bearing S180 tumor which grew to a leg diameter of 10–15 mm. The final solution was diluted to a concentration of 7.4 MBq/mL with saline. Then 0.1 mL of the diluted tracer solution was injected via a tail vein of mice, weighing approximately 20–25 g each (four groups each of five mice). The mice were sacrificed by decapitation at 0.5, 1, 2, 4 h post-injection. The organs of interested were weighted and counted, and the average percent values of the administrated dose/organ (%ID/g) were calculated. Corrections were made for background radiation and physical decay during experiment. All biodistribution studies were carried out in compliance with the national laws related to the conduct of animal experimentation.

Results and discussion

Preparation and structure confirmation of unlabeled HYNIC–MN

HYNIC–MN, the precursor of ^{99m}Tc–HYNIC–MN, was synthesized by the coupling of the carboxyl group of Boc–HYNIC with the amino group of the MN derivative and the subsequent deprotection of the Boc group. The reaction was schematically shown in Scheme 1. All the intermediates and product HYNIC–MN were characterized by ^{1}H NMR and MS.

Labeling of HYNIC–MN

^{99m}Tc–HYNIC–MN was prepared by a one-pot reaction of HYNIC–MN with $^{99m}TcO_4^-$, tricine, and EDDA in the presence of $SnCl_2$. The radiochemical purity of ^{99m}Tc–HYNIC–MN was more than 95%.

Radiochemical purity analysis

The radiochemical purity of the complex was routinely checked by TLC and HPLC. By TLC, in saline, the free $^{99m}TcO_4^-$ and $^{99m}TcO_2 \cdot nH_2O$ remained near the origin with $R_f = 0.0$–0.1, while ^{99m}Tc–HYNIC–MN migrated with the solvent front with $R_f = 0.8$–1.0. An HPLC radiochromatogram was presented in Fig. 1. It was observed that the retention time of $^{99m}TcO_4^-$ was 5.0 min, while that of ^{99m}Tc–HYNIC–MN was found to be 13.6 min. Single peak suggested only one product (^{99m}Tc–HYNIC–MN) was formed. The mean radiochemical purity of the product was over 95% immediately after the preparation.

Stability test

The stability of ^{99m}Tc–HYNIC–MN was studied in order to determine the suitable time for injection to avoid the formation of the undesired products. These undesired radioactive products may be accumulated in non-target organs. Table 1 showed the stability of ^{99m}Tc–HYNIC–MN up to 6 h. It showed the radiochemistry purity was more than 90% after 6 h, which indicated the complex was stable in the reaction mixture at room temperature.

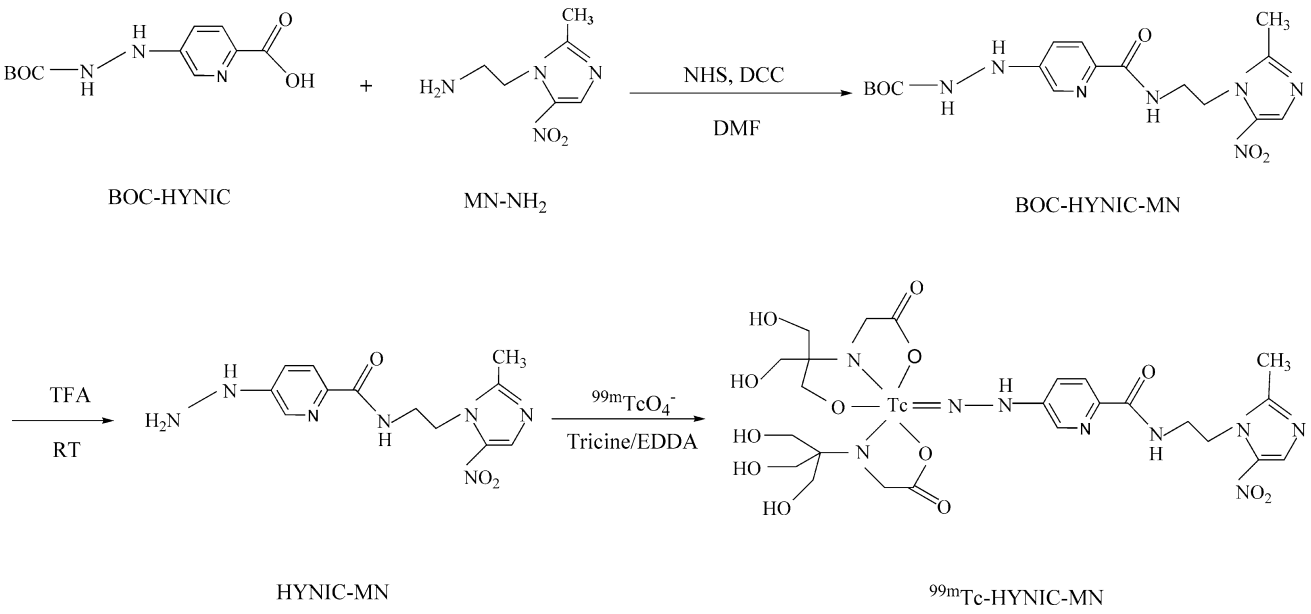

Scheme 1 Synthesis of HYNIC–MN and preparation procedure of ^{99m}Tc–HYNIC-MN

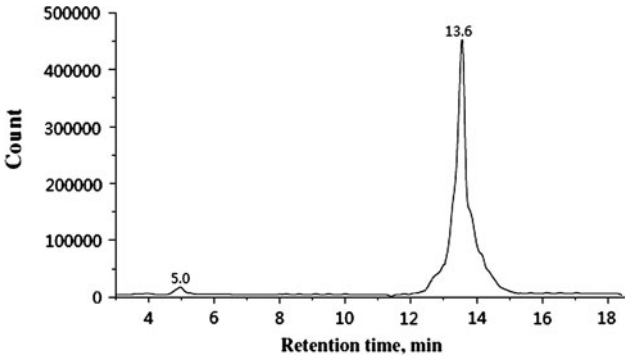

Fig. 1 HPLC radiochromatogram of ^{99m}Tc–HYNIC–MN

Table 1 The in vitro stability of ^{99m}Tc–HYNIC–MN

Time post labeling (h)	^{99m}Tc–HYNIC–MN
1	95.7 ± 1.6
2	95.1 ± 1.2
3	94.5 ± 1.3
4	94.8 ± 1.7
5	94.2 ± 1.3
6	94.3 ± 1.2

Mean ± SD (mean of three experiments). Reaction condition: 10 μg HYNIC-MN, 60 mg tricine, 5 mg EDDA, 1 mL Na^{99m}TcO$_4$, pH 7 and 25 μg $SnCl_2$ solution, 100 °C for 15 min. The reaction mixture was kept at room temperature (25 °C) after preparation

Determination of the partition coefficient (log *P*) for the complex

The partition coefficient (log *P*) value of ^{99m}Tc–HYNIC–MN was −1.68, suggesting it was hydrophilic.

Paper electrophoresis

The electrophoresis results showed that the ^{99m}Tc–HYNIC–MN complex remained at the point of spotting (percentage of radioactivity >90%), suggesting it was a neutral complex.

Cellular accumulation

The effect of anoxic or aerobic conditions on the accumulation of ^{99m}Tc–HYNIC–MN in S180 cells as a function of time was illustrated in Fig. 2. From Fig. 2, it can be seen that the uptake of ^{99m}Tc–HYNIC–MN in anoxic cells was obviously higher than that in aerobic cells, which suggested that ^{99m}Tc–HYNIC–MN had a certain hypoxic selectivity.

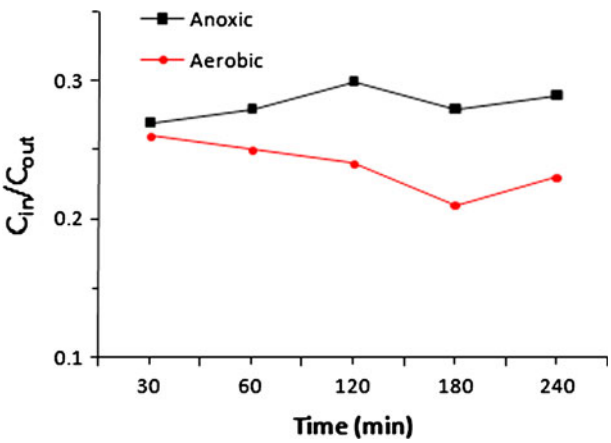

Fig. 2 The accumulation of ^{99m}Tc–HYNIC–MN in anoxic and aerobic S180 cells as a function of time

Table 2 Biodistribution of ^{99m}Tc–HYNIC–MN in normal mice (%ID/g)

Tissues	0.5 h	1.0 h	2.0 h	4.0 h
Heart	0.32 ± 0.05	0.16 ± 0.02	0.10 ± 0.02	0.09 ± 0.01
Liver	1.39 ± 0.13	1.07 ± 0.18	1.04 ± 0.15	0.96 ± 0.17
Spleen	0.46 ± 0.06	0.41 ± 0.06	0.47 ± 0.08	0.44 ± 0.09
Lung	0.89 ± 0.13	0.55 ± 0.04	0.30 ± 0.07	0.16 ± 0.03
Kidney	2.65 ± 0.60	2.06 ± 0.18	1.55 ± 0.08	0.92 ± 0.12
Bone	0.47 ± 0.07	0.44 ± 0.24	0.17 ± 0.04	0.14 ± 0.02
Intestine	1.03 ± 0.23	1.14 ± 0.24	1.08 ± 0.45	0.21 ± 0.02
Muscle	0.32 ± 0.07	0.21 ± 0.04	0.19 ± 0.07	0.06 ± 0.01
Blood	0.73 ± 0.27	0.25 ± 0.05	0.10 ± 0.02	0.03 ± 0.01

All data are the mean percentage ($n = 5$) of the injected dose of ^{99m}Tc–HYNIC–MN per gram of tissue, ± the standard deviation of the mean

Table 3 Biodistribution of ^{99m}Tc–HYNIC–MN in mice bearing S180 tumor (%ID/g)

Tissues	0.5 h	1.0 h	2.0 h	4.0 h
Heart	0.27 ± 0.09	0.19 ± 0.05	0.05 ± 0.01	0.03 ± 0.01
Liver	0.49 ± 0.10	0.34 ± 0.14	0.12 ± 0.02	0.12 ± 0.02
Spleen	0.22 ± 0.05	0.12 ± 0.02	0.06 ± 0.02	0.05 ± 0.01
Lung	0.70 ± 0.18	0.35 ± 0.15	0.07 ± 0.01	0.05 ± 0.01
Kidney	2.71 ± 0.64	1.62 ± 0.57	0.57 ± 0.19	0.42 ± 0.06
Bone	0.28 ± 0.04	0.24 ± 0.09	0.13 ± 0.06	0.15 ± 0.07
Intestine	1.58 ± 0.51	0.56 ± 0.25	0.28 ± 0.08	0.27 ± 0.17
Muscle	0.26 ± 0.08	0.28 ± 0.17	0.12 ± 0.08	0.05 ± 0.02
Tumor	0.81 ± 0.18	0.35 ± 0.08	0.29 ± 0.02	0.22 ± 0.01
Blood	0.73 ± 0.27	0.23 ± 0.04	0.03 ± 0.01	0.01 ± 0.00
T/M	3.12	1.25	2.42	4.40
T/B	1.11	1.52	9.67	22.00

All data are the mean percentage ($n = 5$) of the injected dose of ^{99m}Tc–HYNIC–MN per gram of tissue, ± the standard deviation of the mean

T/M tumor-to-muscle, *T/B* tumor-to-blood

Biodistribution studies in mice

The biodistribution of ^{99m}Tc–HYNIC–MN in normal mice was presented in Table 2. The data showed that the clearance of the tracer from the blood was quickly, from 0.73 ± 0.27%ID/g at 0.5 h to 0.10 ± 0.02%ID/g at 2 h post-injection. This compound was excreted through the kidneys. The uptakes of other organs (bone, muscle, lung, heart, and spleen) were within the normal values.

The biodistribution of ^{99m}Tc–HYNIC–MN in S180 tumor-bearing mice was shown in Table 3. As described in Table 3, ^{99m}Tc–HYNIC–MN had a high uptake at the site of tumor and good target/non-target ratio. The tumor/blood and tumor/muscle ratios increased from 1 to 4 h post injection. The kidney uptake was much higher than the hepatic. Early renal activity reflects urinary elimination of this complex. The uptake of the tracer in bone, muscle, lungs, heart, and spleen was similar to the uptake of the same organs in normal mice.

The comparison of biodistribution of ^{99m}Tc–HYNIC–MN with some reported hypoxia imaging agents in mice bearing tumor was shown in Table 4. As seen from Table 4, ^{99m}Tc–HYNIC–MN exhibited the lowest tumor uptake, but it had the highest T/B ratio (9.67 at 2 h p. i.) among the five complexes. ^{99m}Tc–HYNIC–MN had a good T/M ratio (2.42 at 2 h p. i.), but which was lower than that of the other four complexes. A decrease of T/B ratio in the order was observed: ^{99m}Tc–HYNIC–MN > ^{99m}Tc–N2IPA > ^{99m}Tc–DMSAme = ^{99m}Tc–MNZ–xanthate > ^{99m}Tc–BMS181321. Compared with ^{99m}Tc–DMSAme, the T/B ratio of ^{99m}Tc–HYNIC–MN (9.67 at 2 h p. i.) was much higher and the T/M ratio (2.42 at 2 h p. i.) was very close, which suggested that the clearance of ^{99m}Tc–HYNIC–MN (using HYNIC as bifunctional chelator) from the blood was obviously faster than that of ^{99m}Tc–DMSAme (using DMSA as bifunctional chelator). Also, the biodistribution of ^{99m}Tc–HYNIC–MN in tumor-bearing mice pointed to the possibility of the use of this tracer as tumor hypoxia imaging agent. However, many biological studies are required to establish these findings as the examination of the tracer in vitro preparation of hypoxic tissue and the quantitative determination of the tissue uptake of this tracer.

Conclusion

The novel HYNIC-conjugated metronidazole ligand HYNIC–MN had been successfully synthesized and

Table 4 Comparison of biodistribution of ^{99m}Tc–HYNIC–MN with some reported hypoxia imaging agents

Complex	^{99m}Tc–HYNIC–MN	^{99m}Tc–DMSAme	^{99m}Tc–N2IPA	^{99m}Tc–BMS181321	^{99m}Tc–MNZ–xanthate
Animal	Kunming mice	Kunming mice	Kunming mice	C3H mice	Swiss mice
Tumor type	S 180 tumor	S 180 tumor	S 180 tumor	Fibrosarcoma	Fibrosarcoma
Time p. i. (h)	2	2	2	2	2
Tumor uptake (%ID/g)	0.29 ± 0.02	1.54 ± 0.26	0.49 ± 0.07	0.55 ± 0.08	1.36 ± 0.29
T/M ratio	2.42	2.49	6.66	2.63	3.32
T/B ratio	9.67	0.62	1.00	0.31	0.62
Reference	Present study	12	6	8	8

^{99m}Tc–HYNIC–MN was prepared in high yields using tricine and EDDA as coligands. ^{99m}Tc–HYNIC–MN showed a certain hypoxic selectivity. The high tumor uptake, good retention and high target to non-target activity ratios of the ^{99m}Tc–HYNIC–MN in tumor-bearing mice exhibited favorable properties, suggesting that it could be potentially useful for tumor hypoxia imaging agent.

Acknowledgments The work was financially supported by the Fundamental Research Funds for the Central Universities of China (FRF-BR-09-006A) and by the International Science and Technology Cooperation Program of China (ISTCP) (2008AR), the Ministry of Science and Technology of the People's Republic of China. The radiochemical data were acquired at Key Laboratory of Radiopharmaceuticals (Beijing Normal University), Ministry of Education. The authors thank Dr. Zhang Shijian for his help with the animal experiments.

References

1. Chapman JD (1991) Radiother Oncol 20:13–19
2. Gatenby RA, Kessler HB, Roeenblum JS, Coia LR, Moldofsky PJ, Harz WH (1988) Int J Radiat Oncol Biol Phys 14:831–838
3. Hay MP, Wilson WR, Moselen JW, Palmer BD, Denny WA (1994) J Med Chem 37:381–391
4. Cook GJR, Fogelman I (1998) Eur J Nucl Med 25:335–357
5. Nunn A, Linder K, Strauss HW (1995) Eur J Nucl Med 22: 265–280
6. Chu TW, Li RJ, Hu SW, Liu XQ, Wang XY (2004) Nucl Med Biol 31:199–203
7. Kong DJ, Lu J, Ye SZ, Wang XB (2007) J Labelled Comp Radiopharm 50:1137–1142
8. Mallia MB, Mathur A, Subramanian S, Banerjee S, Sarma HD, Venkatesh M (2005) Bioorg Med Chem Lett 15:3398–3401
9. Mallia MB, Subramanian S, Banerjee S, Sarma HD, Venkatesh M (2006) Bioorg Med Chem 14:7666–7670
10. Mallia MB, Subramanian S, Mathur A, Sarma HD, Venkatesh M, Banerjee S (2008) Bioorg Med Chem Lett 18:5233–5237
11. Zhang Y, Chu TW, Gao XG, Liu XQ, Yang Z, Guo ZQ, Wang XY (2006) Bioorg Med Chem Lett 16:1831–1833
12. Zhang JB, Yu Q, Huo JF, Pang Y, Yang S, He YI, Tang TT, Yang CC, Wang XB (2010) J Radioanal Nucl Chem 283:481–485
13. Liu S, Edwards DS, Barrett JA (1997) Bioconjug Chem 8: 621–636
14. Abrams MJ, Juweid M, TenKate CI, Schwartz DA, Hauser MM, Gaul FE, Fuccello AJ, Rubin RH, Strauss HW, Fischman AJ (1990) J Nucl Med 31:2022–2028
15. Ohtsuki K, Akashi K, Aoka Y, Blankenberg FG, Kopiwoda S, Tait JF, Strauss HW (1999) Eur J Nucl Med 26:1251–1258
16. Steffens MG, Oosterwijk E, Kranenborg MHGC, Manders JMB, Debruyne FMJ, Corstens FHM, Boerman OC (1999) J Nucl Med 40:829–836
17. Ono M, Arano Y, Mukai T, Fujioka Y, Ogawa K, Uehara T, Saga T, Konishi J, Saji H (2001) Nucl Med Biol 28:215–224